RESEARCH ARTICLE

Figures and figure supplements

Bidirectional regulation of postmitotic H3K27me3 distributions underlie cerebellar granule neuron maturation dynamics

Vijyendra Ramesh and Fang Liu *et al*.

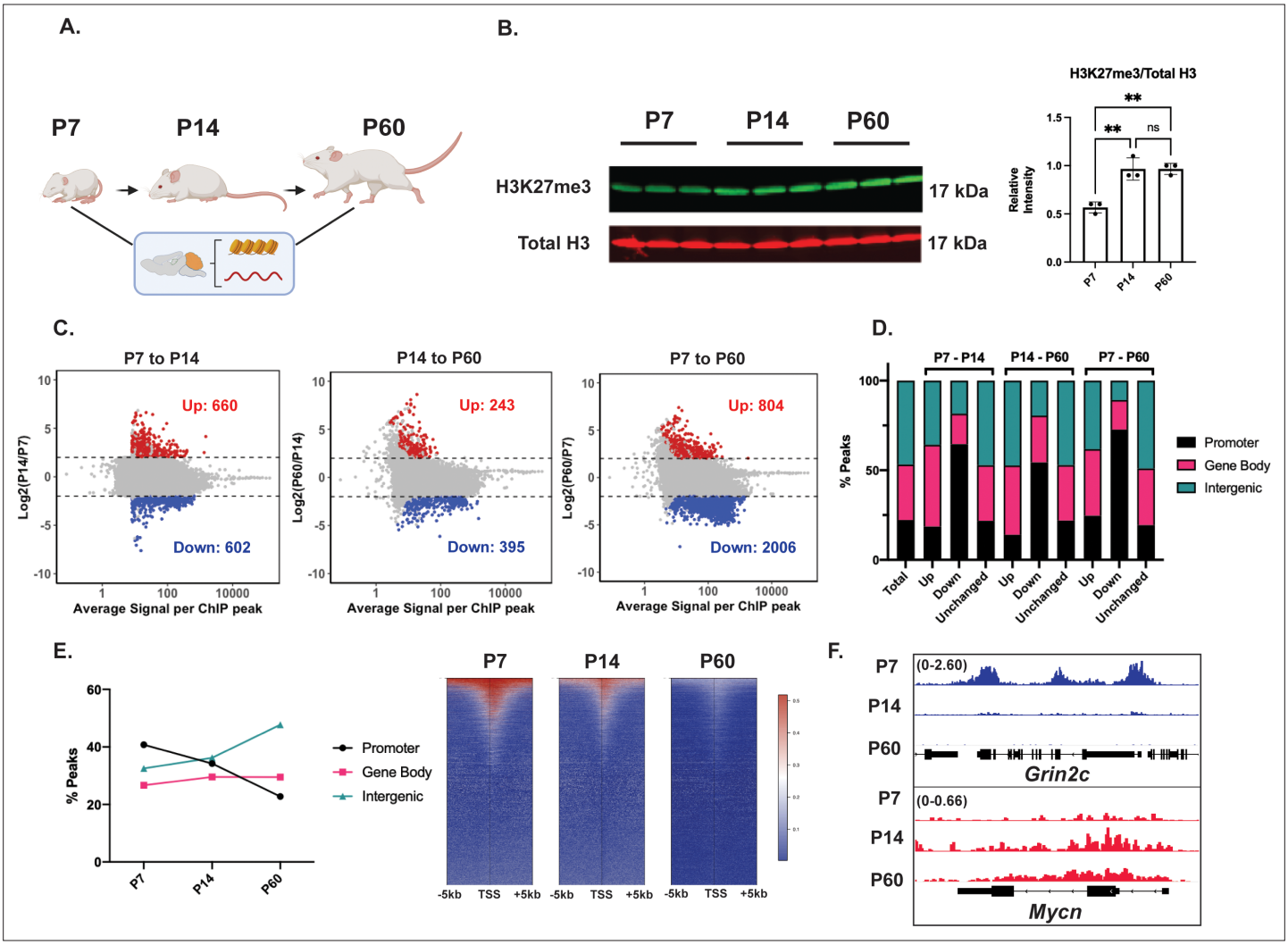

Figure 1. The maturing mouse cerebellum undergoes a genome-wide redistribution of histone H3 lysine 27 trimethylation (H3K27me3). (**A**) Mice were sacrificed at postnatal days 7, 14, and 60 after which cerebellar tissue was dissected out and processed to harvest histones, chromatin, and RNA. (**B**) (Left) Western blot of acid extracted histone from cerebellar tissue for H3K27me3 and total Histone H3 (n=3 biological replicates), (Right) Quantification of Western Blot, one-way ANOVA, ** indicates p<0.005. (**C**) MA plots showing H3K27me3 peaks gained (Up) and lost (Down) throughout cerebellar maturation in vivo (n=3 biological replicates, differential enrichment calculated using DESeq2 package. Up and Down are loci with FDR <0.05 and |L2FC|>2). (**D**) Percentage of differential H3K27me3 peaks between P7-P14, P14-P60, and P7-P60, annotated by genomic region. Annotation performed using ChIPseeker package, TSS +/− 3000 bp; 'Total' represents consensus H3K27me3 peaks across P7, P14, and P60. (**E**) (Left) Percentage of H3K27me3 peaks annotated by genomic region, (Right) Heatmap of H3K27me3 peaks centered around genes with H3K27me3 peaks TSS +/− 5000 *bp*. (**F**) ChIP-seq tracks for example 'Down' gene *Grin2c* (Upper) and 'Up' gene *Myc* (lower). The numbers at the top of each track indicate the y-axis scale, which is fixed for all tracks in the same set. Source Data.

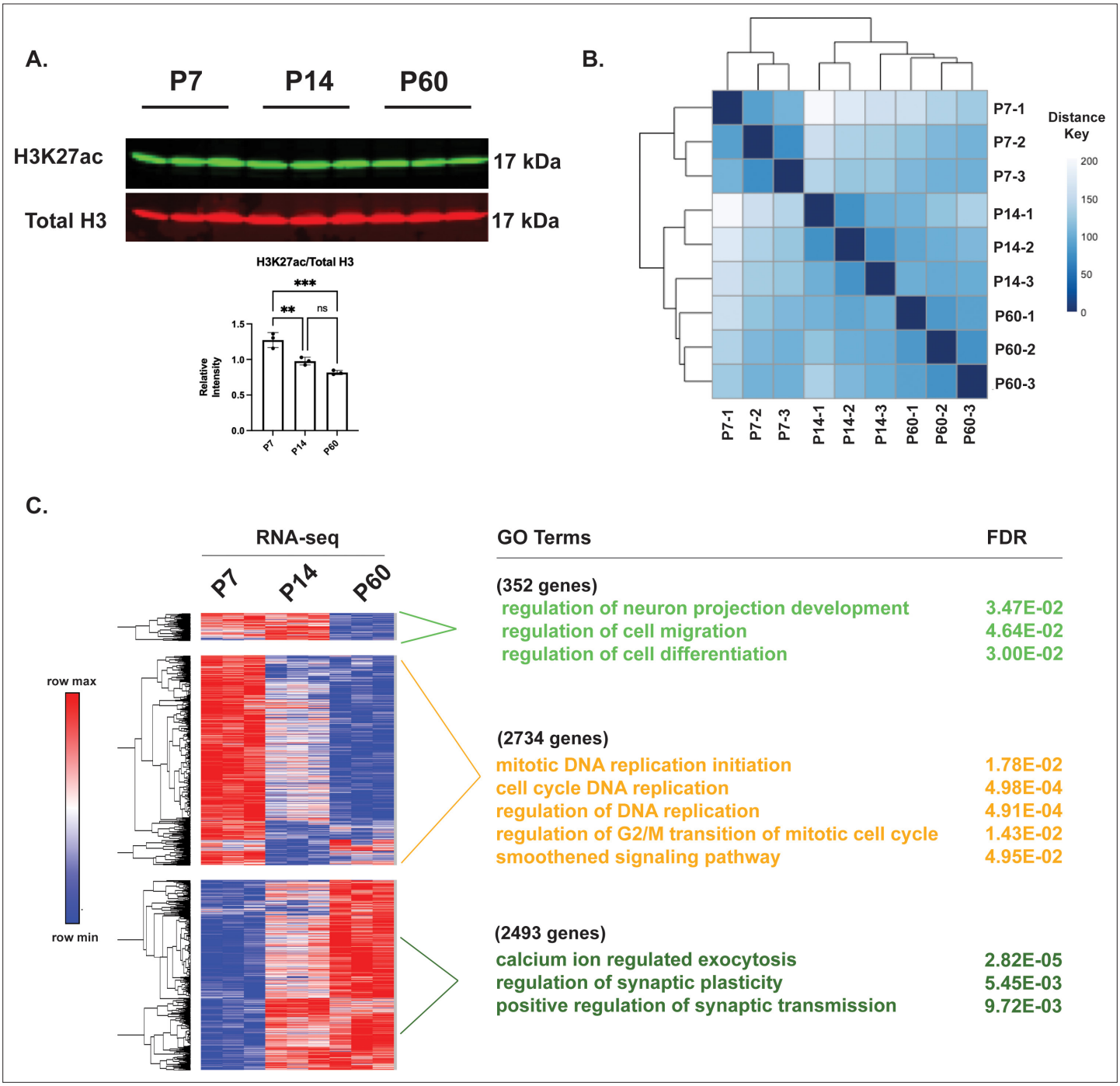

Figure 1—figure supplement 1. Histone H3 lysine 27 trimethylation (H3K27me3) ChIP-seq and RNA-seq profile of the developing cerebellum in vivo. (**A**) (upper) Western blot of acid extracted histone from cerebellar tissue for H3K27ac and total Histone H3 (n=3 biological replicates), (lower) Quantification of Western Blot, one-way ANOVA, ** indicates p<0.005, *** indicates p<0.001. (**B**) Sample to Sample Distance plot for H3K27me3 ChIP-seq peaks for P7, P14, and P60 tissues and their three biological replicates. (**C**) (Left) Heatmap of Spearman rank correlated, hierarchically clustered VST-transformed DESeq2-normalized RNA-seq counts for significantly different genes from P7-P60, (Right) Corresponding Gene Ontology (GO) Terms and FDR associated with each cluster.

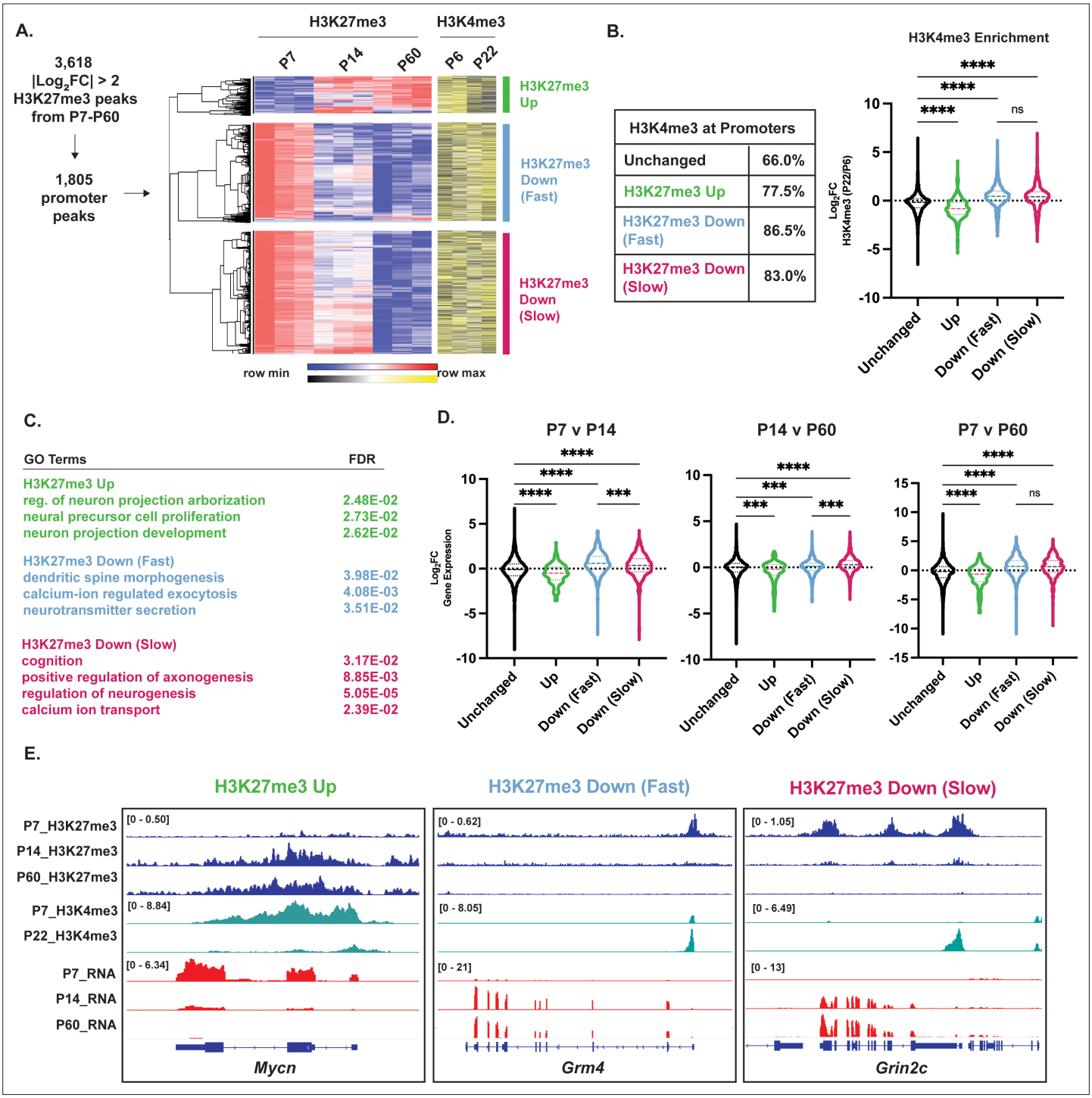

Figure 2. Differential histone H3 lysine 27 trimethylation (H3K27me3) promoters cluster by turnover kinetics and correlate with cerebellar granule neuron (CGN) maturation gene expression. (**A**) Differential H3K27me3 peaks across P7 to P60 were filtered for promoter-associated peaks, followed by the hierarchical clustering with Pearson correlation, of their VST-transformed DESeq2-normalized counts (left) from P7-P60, and corresponding VST-transformed DESeq2-normalized counts for H3K4me3 from P6-P22 (adapted from ***Yamada et al., 2014***). (**B**) (left) Table showing percent overlap of promoters in clusters described in A with promoters with H3K4me3. (right) Violin plot showing the distribution of Log2FC of H3K4me3 (P22/P6) as a function of clustering performed in A, (one-way ANOVA, **** indicates p<0.0001). (**C**) Gene Ontology (GO) Terms associated with the nearest gene and FDR for clusters described in A. (**D**) Violin plot showing the distribution of Log2FC of gene expression, measured by RNA-seq as a function of clustering performed in A, and genes with unchanged H3K27me3 across developmental time (one-way ANOVA, **p<0.005, ***p<0.001, ****p<0.0001). (**E**) Example H3K27me3 (blue) and H3K4me3 (green) ChIP-seq and RNA-seq (red) tracks belonging to CGN maturation genes within clusters described in A, at *Mycn*, *Grm4,* and *Grin2c* loci. The numbers at the top of each track indicate the y-axis scale, which is fixed for all tracks in the same set.

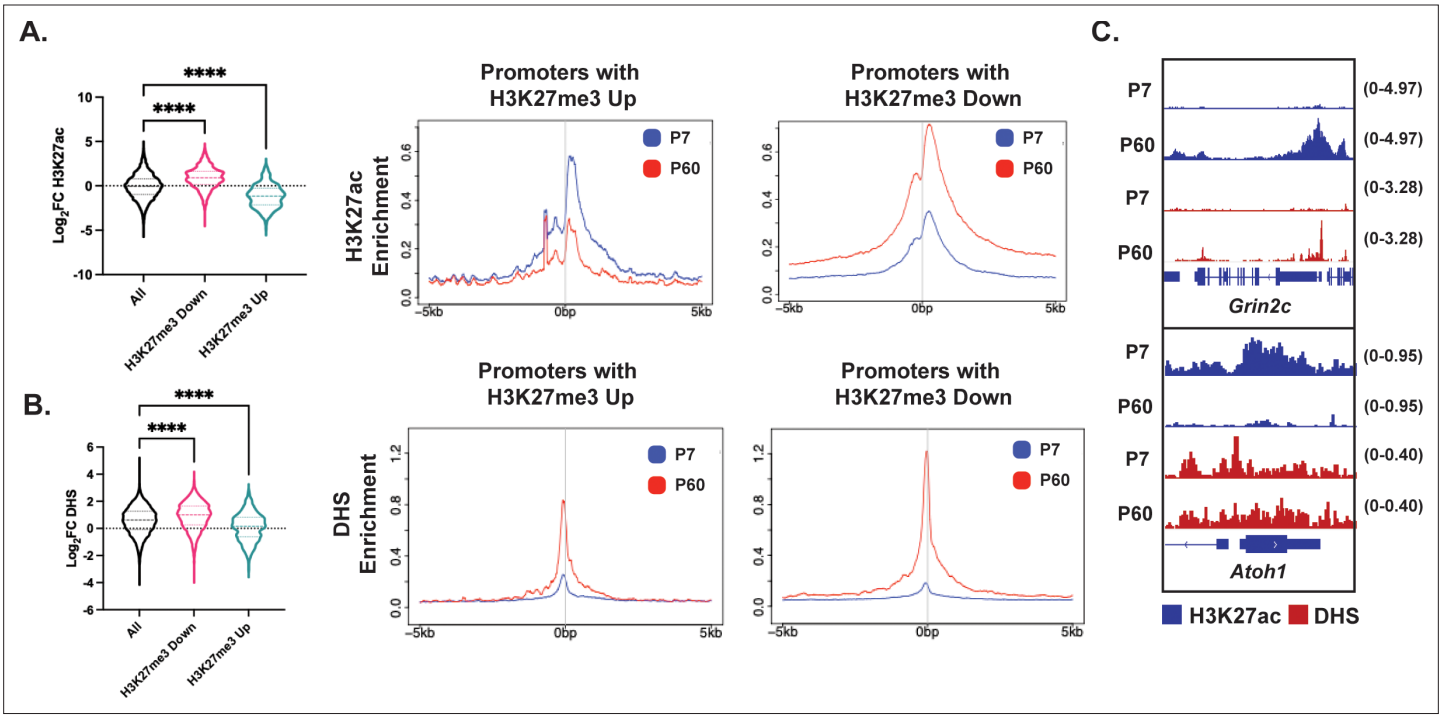

Figure 2—figure supplement 1. Histone H3 lysine 27 trimethylation (H3K27me3) removal is followed by a gain of H3K27ac and chromatin accessibility at gene promoters. (**A**) (Left) Distribution of Log_2Fold Change of H3K27ac enrichment as a function of H3K27me3 Down and H3K27me3 Up described in ***Figure 2*** (one-way ANOVA, **** indicates p<0.0001); and (Right) Metagene plots showing H3K27ac ChIP-seq signal at genes with H3K27me3 Up and H3K27me3 Down. (**B**) (Left) Distribution of Log_2Fold Change of DNase Hypersensitivity as a function of H3K27me3 Down and H3K27me3 Up described in ***Figure 2*** (one-way ANOVA, **** indicates p<0.0001); and (Right) Metagene plots showing DNAse-seq signal at genes with H3K27me3 Up and H3K27me3 Down. (**C**) H3K27ac ChIP-seq and DNAse-seq tracks at P7 and P60 at synaptic gene *Grin2c* (upper), and early gene *Atoh1* (lower).

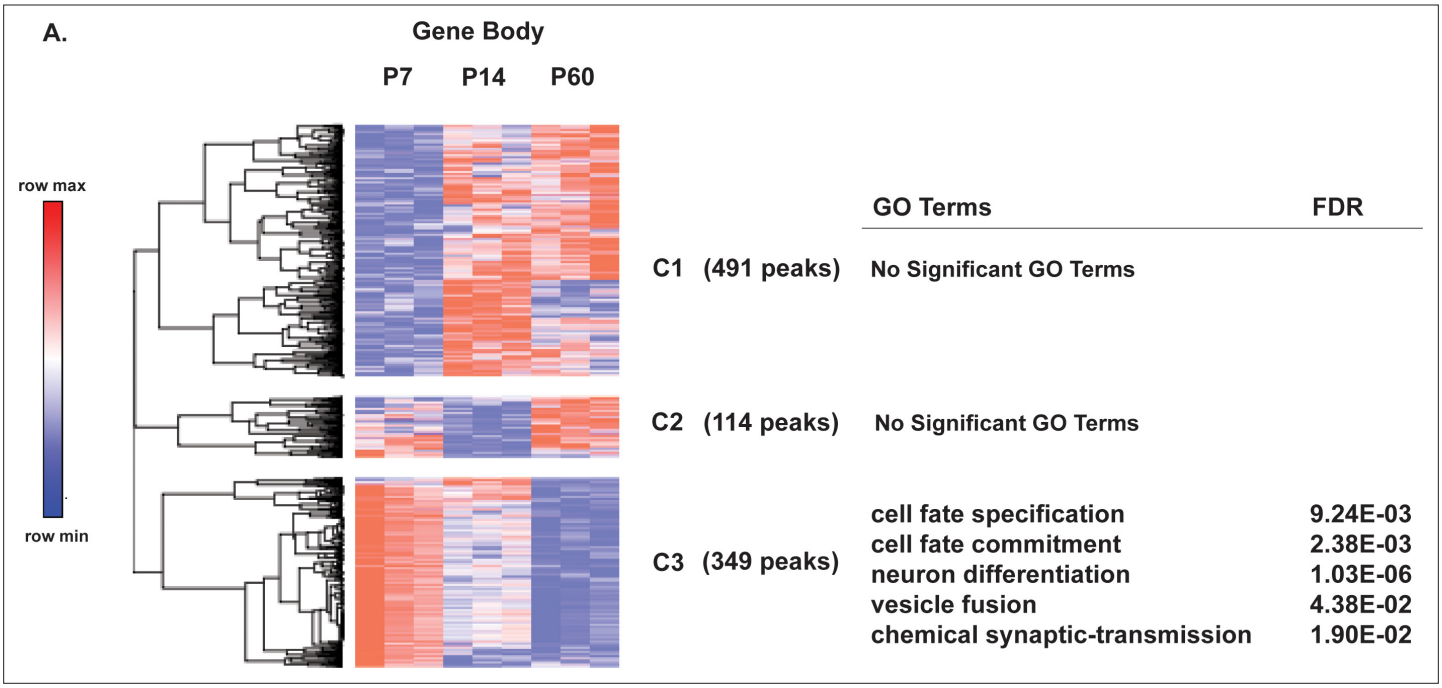

Figure 2—figure supplement 2. Differential histone H3 lysine 27 trimethylation (H3K27me3) enrichment at gene body regions and corresponding GO terms. (**A**) (Left) Heatmap of Spearman rank correlated, hierarchically clustered VST-transformed DESeq2-normalized counts of differential H3K27me3 gene-body peaks from P7-P60, (Right) Corresponding Gene Ontology (GO) Terms and FDR associated with the nearest gene.

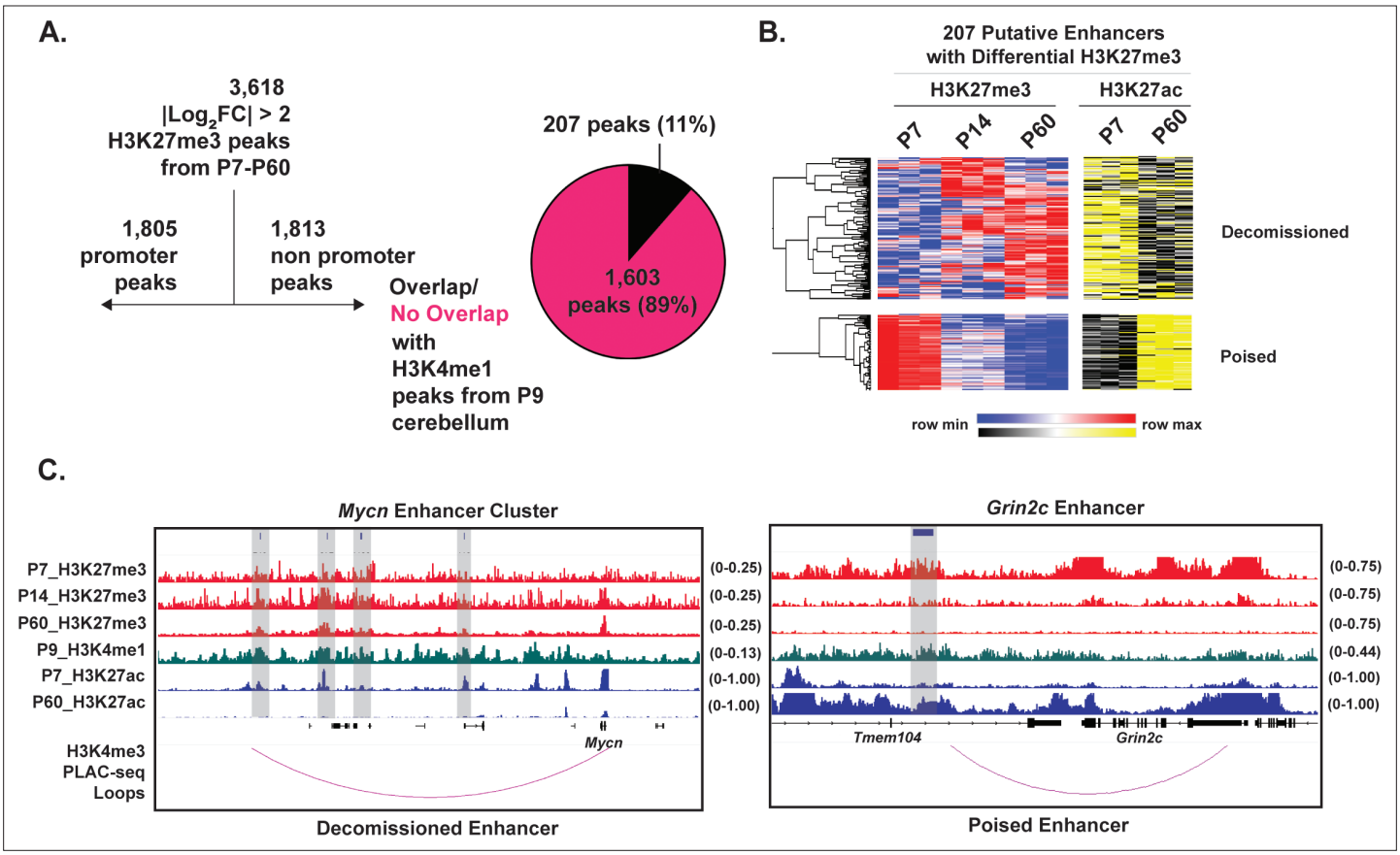

Figure 3. Histone H3 lysine 27 trimethylation (H3K27me3) is bidirectionally regulated at a sparse set of developmentally regulated enhancers. (**A**) Filtering for differential H3K27me3 peaks from P7-14-60 with |Log2FC|>2, for non-promoters (TSS +/− 3 kb), followed by overlap with H3K4me1 peaks obtained from P9 cerebellum from ***Ramirez et al., 2022***, (n=2) biological replicates. (**B**) Heatmap of spearman rank correlated, hierarchically clustered, VST-transformed DESeq2-normalized counts of differential H3K27me3 peaks at putative enhancers (left) from P7-P60, and corresponding VST-transformed DESeq2-normalized counts for H3K27ac from P7-P60 adapted from ***Frank et al., 2015***. (**C**) (Left) Tracks for H3K27me3 (red), H3K4me1 (green) and H3K27ac (blue) and H3K4me3 (purple) PLAC-seq loops from ***Yamada et al., 2019*** at putative enhancer for *Mycn*. (**D**) Same as 'C' but for putative *Grin2c* enhancer. Gray bars indicate putative enhancers. The numbers at the top of each track indicate the y-axis scale, which is fixed for all tracks in the same set.

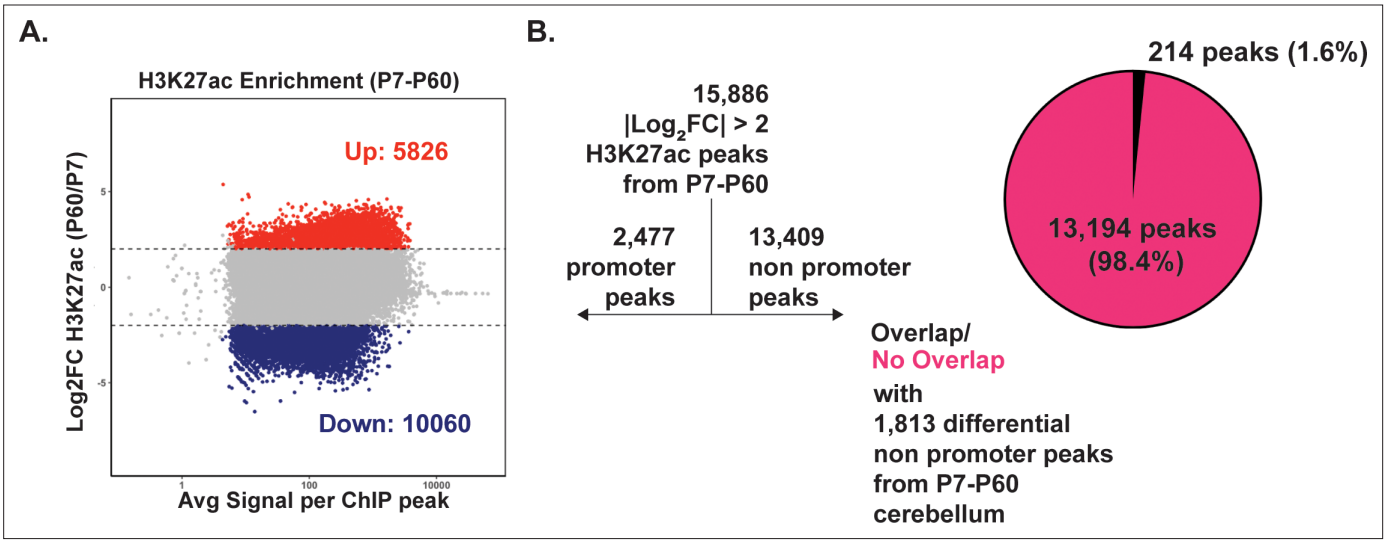

Figure 3—figure supplement 1. Only a subset of differential H3K27ac peaks at non-promoters is also differentially H3K27-trimethylated. (**A**) MA plot describing differential H3K27ac enrichment between P7 and 60 cerebellum. |L2FC >2, FDR <0.05|. Data derived from ***Frank et al., 2015***. (**B**) Filtering differential H3K27ac peaks and computing their overlap with 1,805 differential non-promoter histone H3 lysine 27 trimethylation (H3K27me3) peaks reveals only 1.6% of all H3K27ac peaks are also differential H3K27-trimethylated.

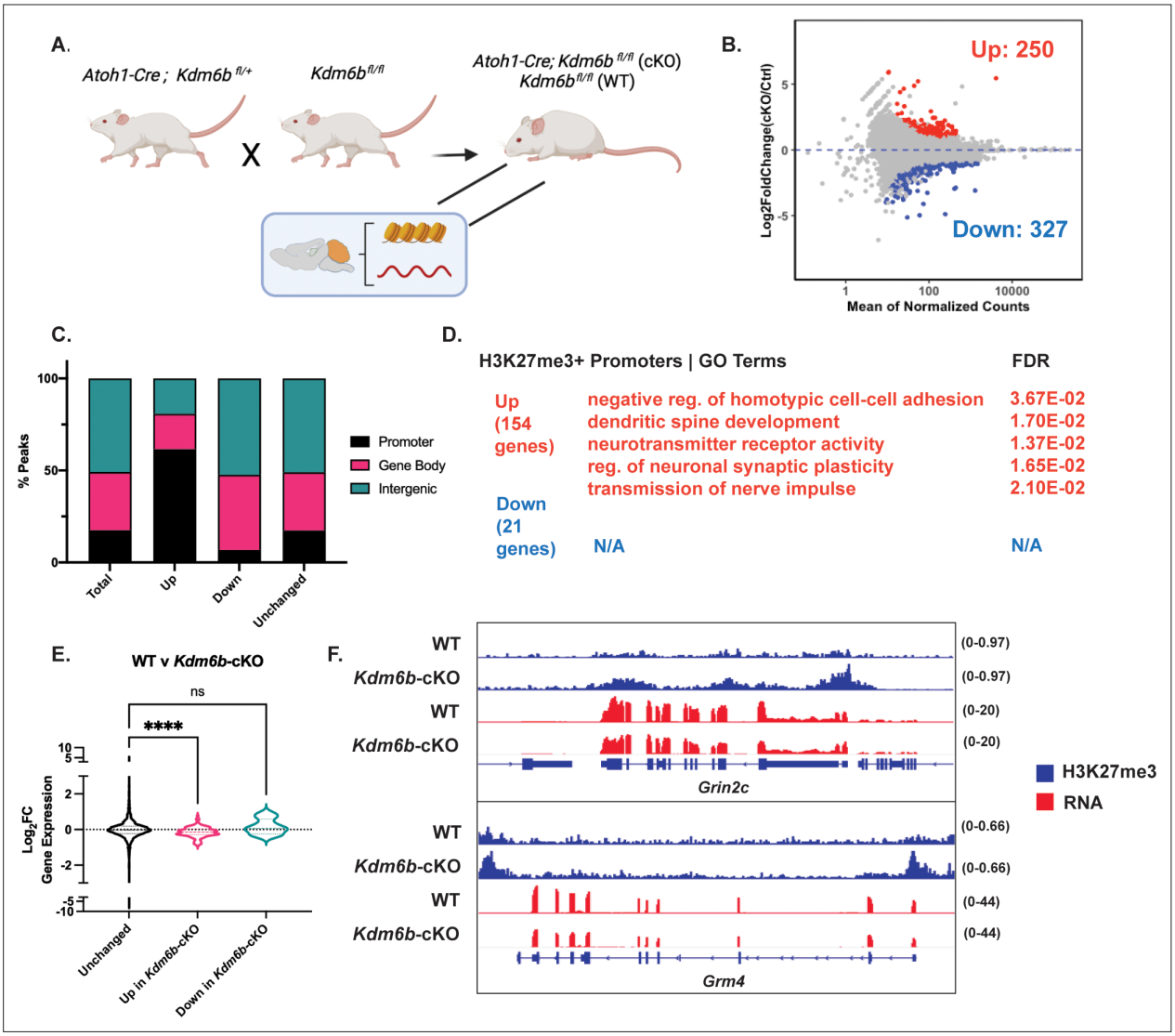

Figure 4. *Kdm6b* knockout in cerebellar granule neuron (CGN) precursors impairs CGN maturation via histone H3 lysine 27 trimethylation (H3K27me3) hypermethylation of CGN maturation gene promoters. (**A**) *Atoh1-Cre; Kdm6b*$^{fl/fl}$ (cKO) and *Kdm6b*$^{fl/fl}$ (WT) mice were generated by crossing *Atoh1-Cre; Kdm6b*$^{fl/+}$ mice to *Kdm6b*$^{fl/fl}$ mice and were sacrificed at P14 for cerebellar tissue harvest and subsequent performing of H3K27me3 ChIP-seq (WT n=2, cKO n=3 biological replicates) and RNA-seq (n=2 biological replicates). (**B**) MA plot showing differential enrichment of genome-wide H3K27me3 peaks between WT and cKO mice (|Log2FC|>1, FDR <0.05). (**C**) Differentially methylated H3K27me3 between WT and cKO annotated by genomic location using ChIPseeker package, TSS +/− 3000 bp. (**D**) Gene Ontology (GO) Terms and FDR for genes nearest gene promoters within H3K27me3 Up and Down (due to *Kdm6b*-cKO) peaks. (**E**) Distribution of Log_2Fold Change Expression (WT v cKO, computed using DESeq2) as a function of unchanged, H3K27me3 Up and H3K27me3 Down genomic promoters between WT and cKO (one-way ANOVA, **** indicates p<0.0001). (**F**) Representative genes containing H3K27me3 (blue) Up genomic promoter peaks *Grin2c* and *Grm4* and corresponding RNA-seq (red) tracks between WT and cKO mice. The numbers to the right of each track indicate the y-axis scale, which is fixed for all tracks in the same set.

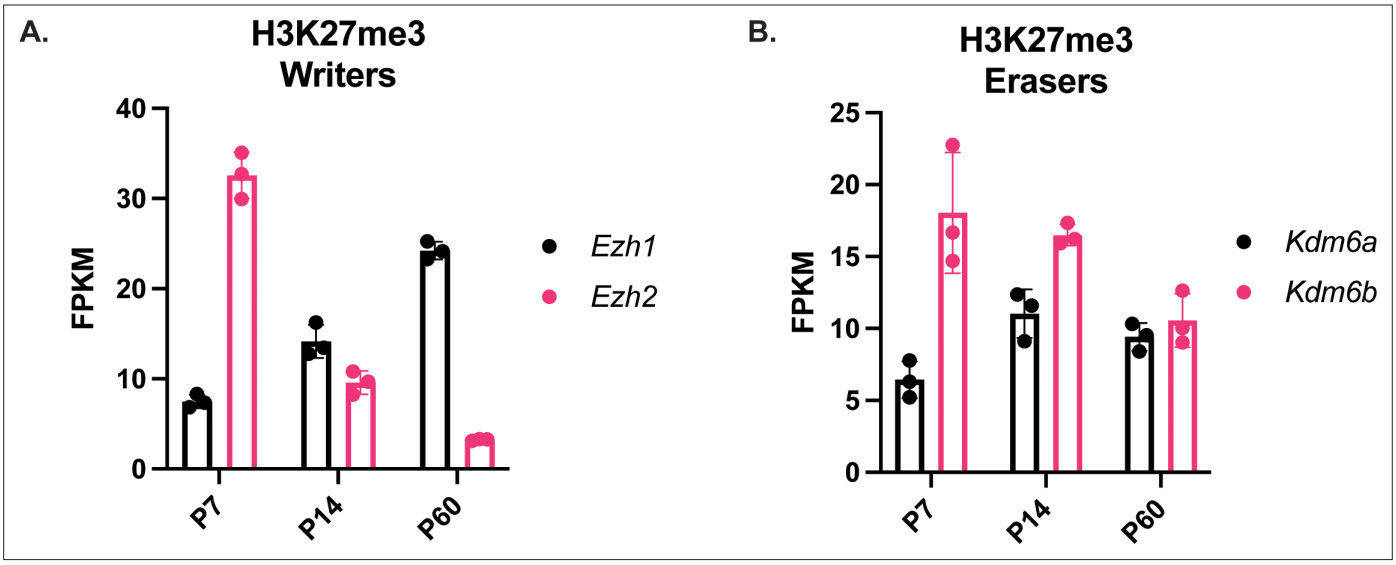

Figure 4—figure supplement 1. Expression of histone H3 lysine 27 trimethylation (H3K27me3) Writers and Erasers in vivo. (**A**) FPKM for H3K27me3 Writers *Ezh1*/2 and (**B**) *Kdm6a/b* obtained from ***Frank et al., 2015***.

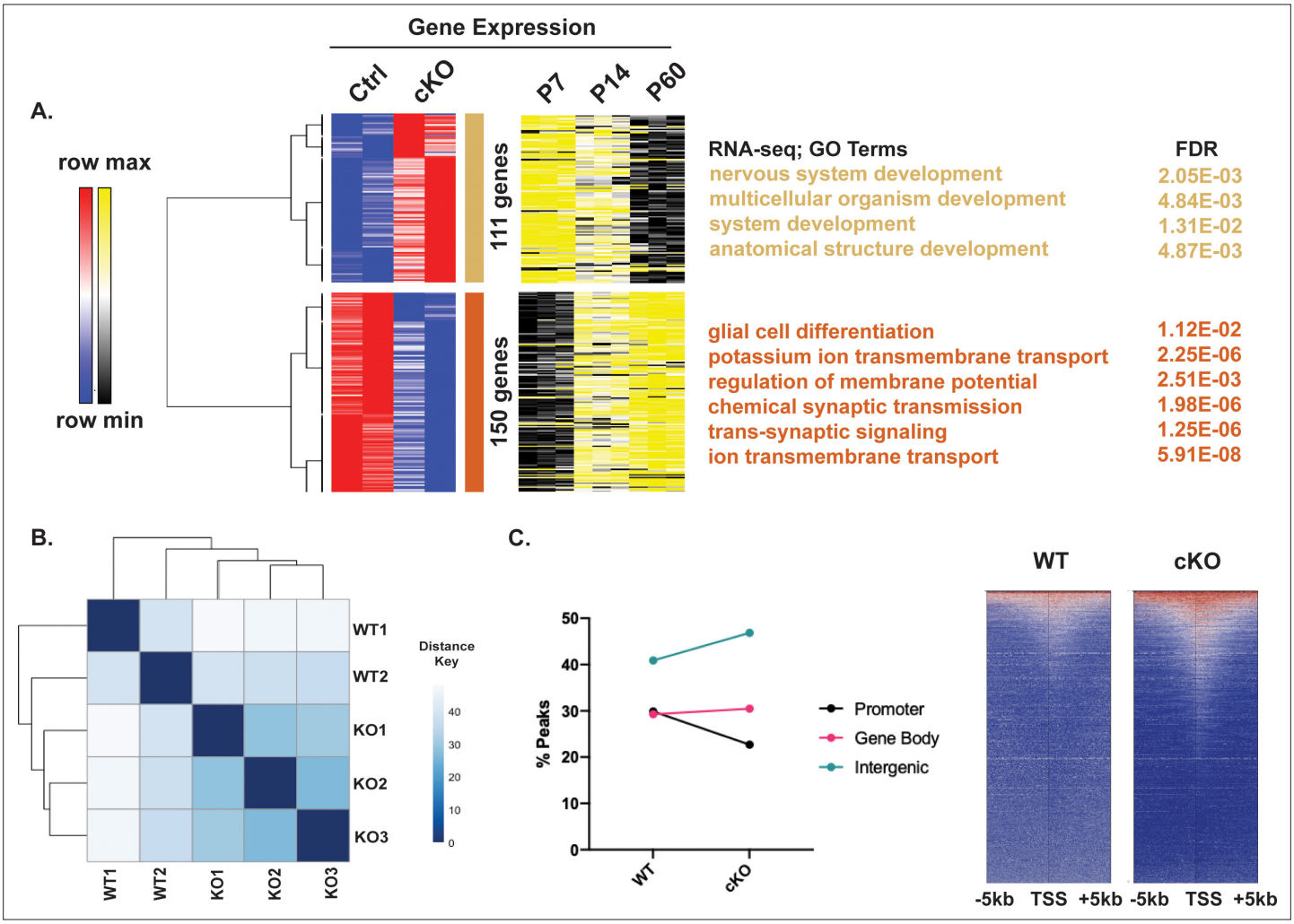

Figure 4—figure supplement 2. *Kdm6b*-cKO in *Atoh1-Cre+* granule neuron precursors (GNPs) Impairs cerebellar granule neuron (CGN) Maturation in vivo. (**A**) (left) Heatmap of Spearman rank correlated, hierarchically clustered VST-transformed DESeq2-normalized RNA-seq counts of differential genes between WT and *Kdm6b*-cKO mice (n=2 biological replicates) and corresponding VST-transformed DESeq2-normalized RNA-seq counts from P7-P60 (right) corresponding Gene Ontology (GO) terms and FDR for those clusters (**B**) Sample to sample distance for histone H3 lysine 27 trimethylation (H3K27me3) ChIP-seq peaks derived from WT and *Kdm6b*-cKO tissue and their biological replicates (WT n=2, cKO n=3 biological replicates). (**C**) (left) Percentage of H3K27me3 peaks annotated by genomic location – promoter, gene body, or distal intergenic region. (right) Heatmap showing H3K27me3 peak coverage around genes with H3K27me3 between WT and cKO tissue with a window of TSS +/− 5 kb.

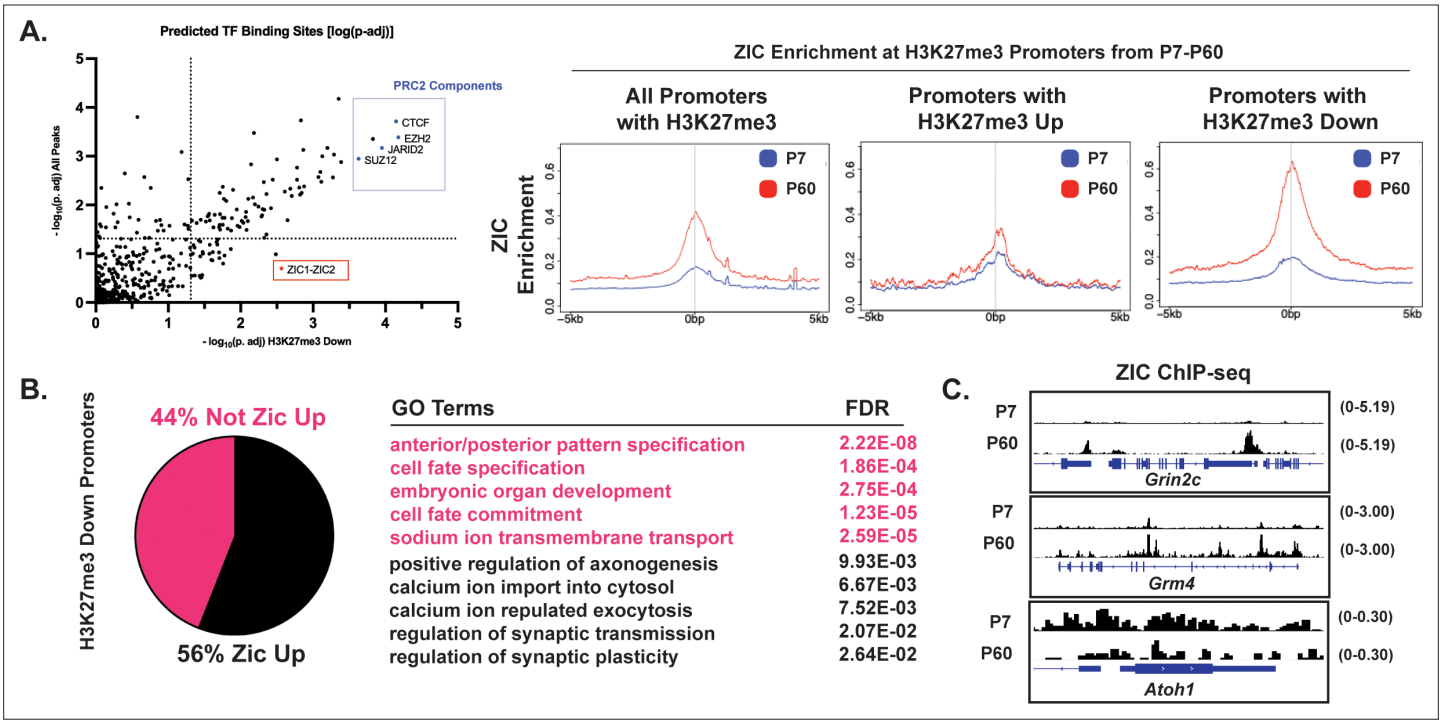

Figure 5. Histone H3 lysine 27 trimethylation (H3K27me3) removal is accompanied by the gain of ZIC at gene promoters. (**A**) (Left) Binding Analysis for Regulation of Transcription (BART) for genes near promoters within H3K27me3 Down peaks (x-axis) and near all H3K27me3 peaks (y-axis) plotted by -$\log_{10}$p-adj. (Right) Metagene plots for ZIC ChIP-seq signal at genes near all promoters with H3K27me3, promoters with H3K27me3 Up, and promoters with H3K27me3 down. (**B**) (Left) Percentage of genes near H3K27me3 Down promoters that are also ZIC1/2 Up (Log_2Fold Change >0, P60/P7, ZIC1/2 ChIP-seq). (Right) Gene Ontology (GO) Terms and FDR for genes nearest to H3K27me3 Down promoter peaks that are also ZIC1/2 Up, and not ZIC1/2 Up. (**C**) ZIC ChIP-seq tracks at P7 and P60 at H3K27me3 Down promoters of Grin2c and Grm4, compared to the early gene Atoh1. The numbers to the right of each track indicate the y-axis scale, which is fixed for all tracks in the same set.

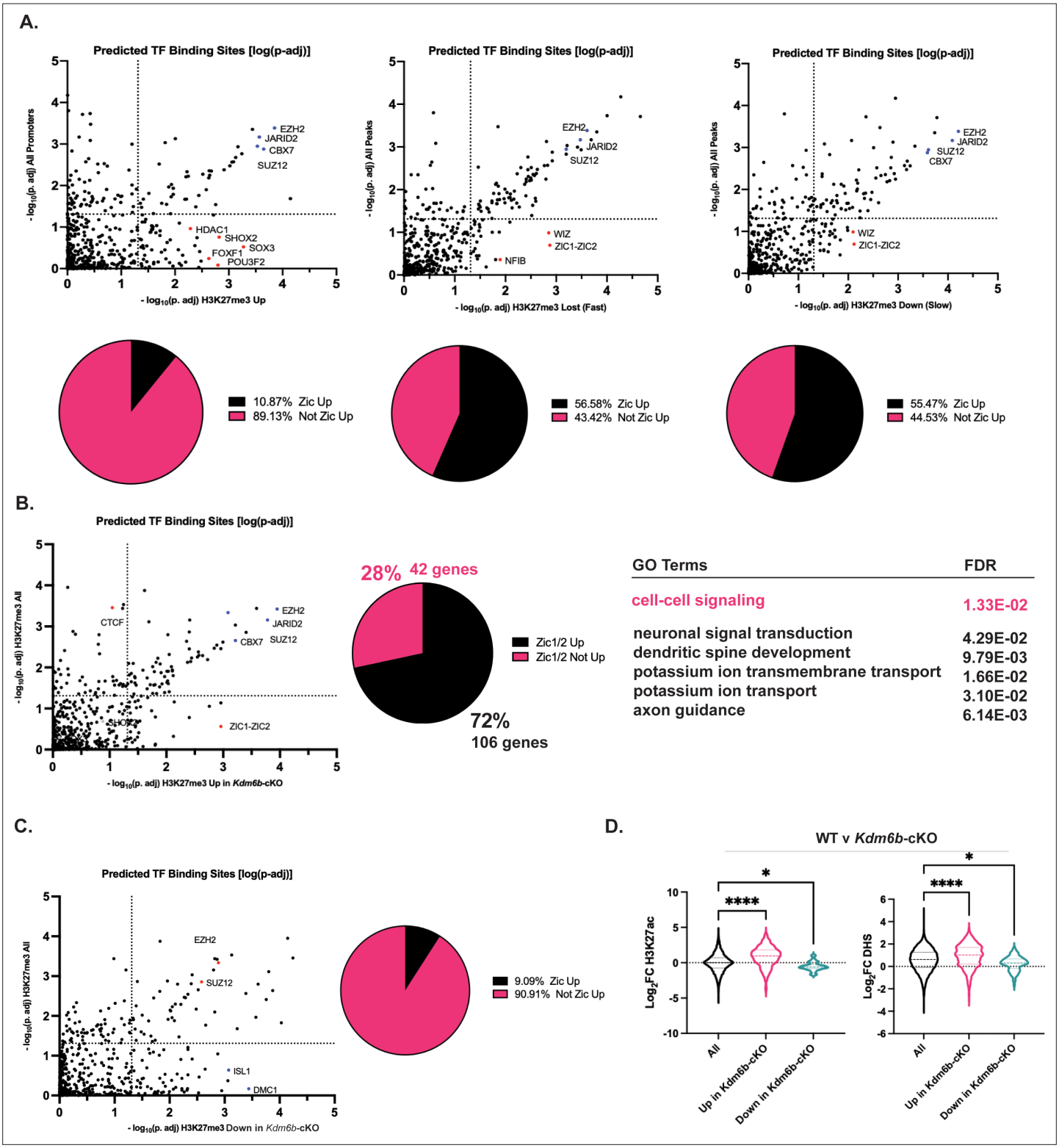

Figure 5—figure supplement 1. Histone H3 lysine 27 trimethylation (H3K27me3) turnover at CGN-maturation gene promoters is associated with gain of ZIC binding. (**A**) (upper) Binding Analysis for Regulation of Transcription (BART) analysis for genes with promoters within H3K27me3 Up, H3K27me3 Down (Fast), and H3K27me3 Down (Slow) clusters described in ***Figure 2A*** versus genes near all H3K27me3 marked promoters plotted as –log10(p-adj). (lower) Overlap between genes with promoters within H3K27me3 Up, H3K27me3 Down (Fast), and H3K27me3 Down (Slow) clusters and ZIC1/2 Up promoter peaks. (**B**) (Left) BART analysis comparing genes with H3K27me3 Up promoters due to *Kdm6b*-cKO described in ***Figure 3***. (Center) Percentage of genes with H3K27me3 Up promoters due to *Kdm6b*-cKO that are also ZIC1/2 Up (Log_2Fold Change >0, P60/P7, ZIC1/2 ChIP-seq). (Right)

Figure 5—figure supplement 1 continued on next page

Figure 5—figure supplement 1 continued

Gene Ontology (GO) Terms and FDR for genes with H3K27me3 Up promoters due to *Kdm6b*-cKO that are also ZIC1/2 Up, and not ZIC1/2 Up. (**C**) BART analysis for genes with H3K27me3-Down promoters due to *Kdm6b*-cKO versus all H3K27me3 promoter peaks plotted as –log10(p-adj), (right) overlap between genes with ZIC1/2 Up promoters. (**D**) Distribution of Log_2Fold Change of H3K27ac enrichment and DNAse Hypersensitivity as a function of 'Up in *Kdm6b*-cKO' and 'Down in *Kdm6b*-cKO' described in ***Figure 3*** (one-way ANOVA, * indicates $p<0.05$, **** indicates $p<0.0001$).

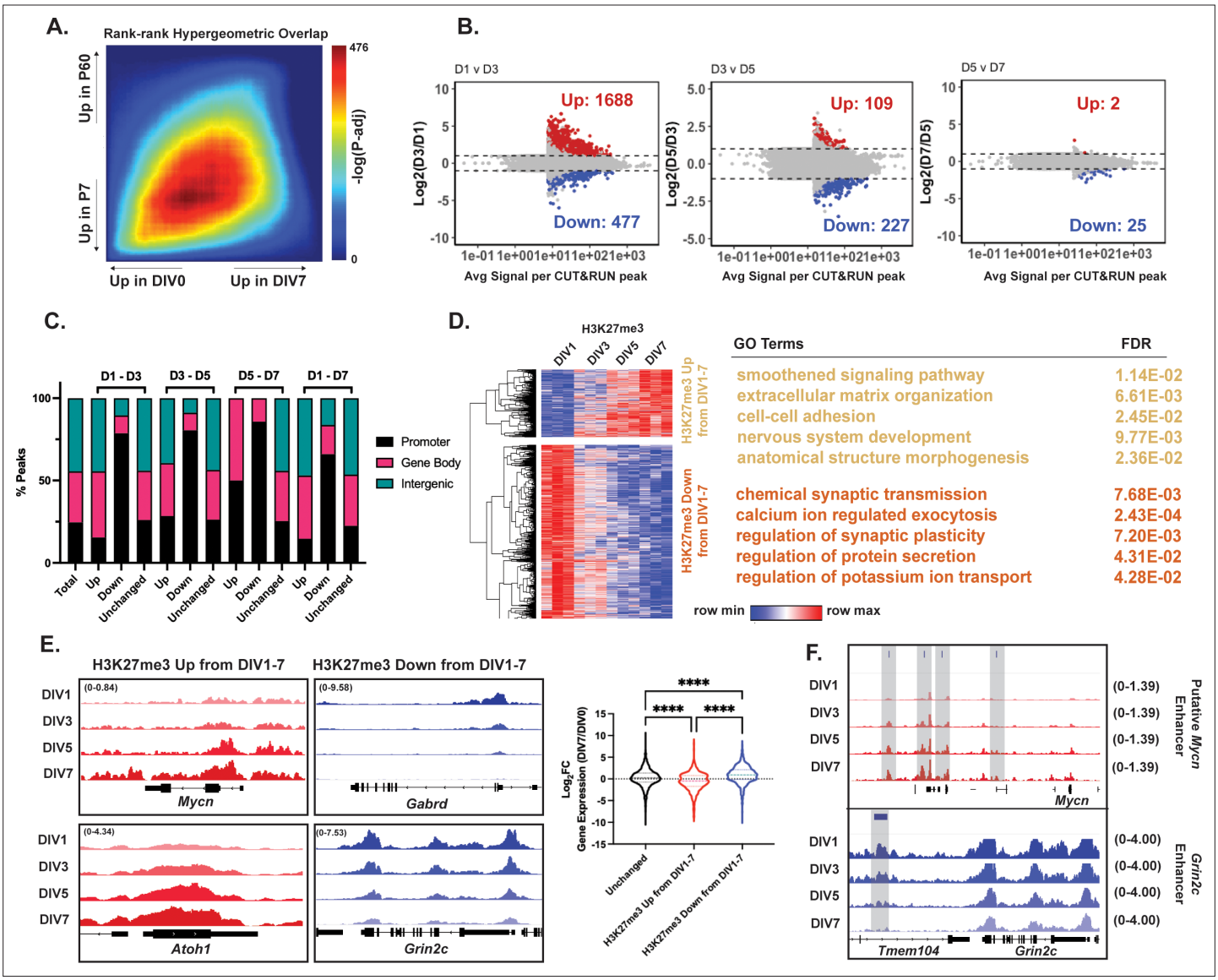

Figure 6. Cerebellar granule neurons (CGNs) differentiating in culture reveal temporal dynamics of histone H3 lysine 27 trimethylation (H3K27me3) changes. (**A**) Rank-rank hypergeometric overlap (RRHO) plot displaying concordance of differential gene expression measured by RNA-seq for P7-P60 cerebellum (y-axis), and cultured granule neurons for DIV0-7 (x-axis). (**B**) Differentially methylated H3K27me3 CUT&RUN peaks between DIV1-3, DIV3–5, DIV5–7, and DIV1–7. (**C**) Percentage of differential H3K27me3 CUT&RUN peaks between DIV1-3, DIV3-5, DIV5-7, and DIV1-7 annotated by genomic region (Annotation performed using ChIPseeker package, TSS +/− 3000 bp). 'Total' represents consensus H3K27me3 peaks across DIV1, DIV3, DIV5, and DIV7 combined. (**D**) (Left) Heatmap of spearman rank correlated, hierarchically clustered VST-transformed DESeq2-normalized counts of H3K27me3 CUT&RUN peaks filtered for differential promoter peaks from DIV1-7 with |Log2FC|>1 and p-adj <0.05, (Right) Corresponding Gene Ontology (GO) Terms and FDR associated with the nearest gene. (**E**) CUT&RUN tracks for H3K27me3 at example genes from 'H3K27me3 Up from DIV1-7' cluster, *Mycn* and *Atoh1*, and 'H3K27me3 Down from DIV1-7' cluster, *Gabrd*, and *Grin2c*; (right) Violin plot showing the distribution of Log2FC of gene expression measured by RNA-seq between DIV0 and DIV7 CGNs as a function of clustering performed in D (one-way ANOVA, **** indicates p<0.0001). (**F**) Tracks for H3K27me3 measured by CUT&RUN at putative postmitotic cerebellar enhancers described in ***Figure 2***. Gray bars indicate putative enhancers. The numbers at the top or the right of each track indicate the y-axis scale, which is fixed for all tracks in the same set.

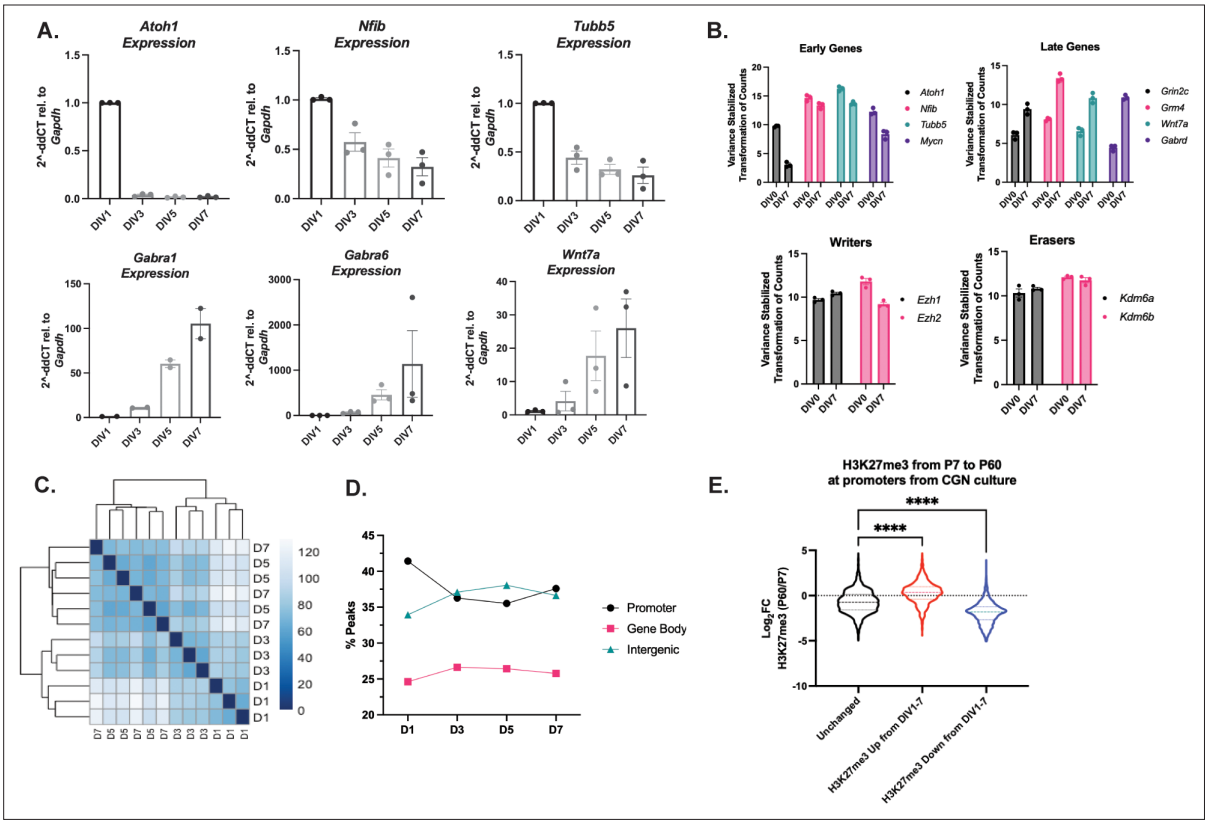

Figure 6—figure supplement 1. CUT&RUN captures genome-wide changes in histone H3 lysine 27 trimethylation (H3K27me3) in cultured cerebellar granule neurons (CGNs). (**A**) RT-qPCR for (top) early genes *Atoh1, Nfib*, and *Tubb5* and (bottom) late genes *Gabra1*, *Wnt7a*, and *Gabra6* (n=2–3 biological replicates). (**B**) (Upper) VST-transformed DESeq2-normalized RNA-seq counts for early genes *Atoh1*, *Nfib*, *Tubb5*, and *Mycn* (left) and late genes *Grin2c*, *Grm4*, *Wnt7a*, and *Gabrd* (right). (Lower) VST-transformed DESeq2-normalized RNA-seq counts for H3K27me3 Writers *Ezh1/2* (left) and *Kdm6a/b* (right). (**C**) Sample-to-sample distance plot for H3K27me3 CUT&RUN peaks from CGNs at DIV1, DIV3, DIV5, and DIV7 and their biological replicates. (**D**) Percentage of H3K27me3 peaks annotated by genomic location – promoter, gene body, or distal intergenic region. (**E**) Violin plot showing the distribution of Log_2FC of H3K27me3 in vivo between P7 and P60 cerebellum as a function of clustering performed in ***Figure 6D*** (one-way ANOVA, * indicates p<0.05; **** indicates p<0.0001).

Figure 7. EZH2 catalytic activity temporally regulates cerebellar granule neuron (CGN) maturation by depositing histone H3 lysine 27 trimethylation (H3K27me3) at early CGN genes. (**A**) (Left) Western blot of acid-extracted histones from CGNs treated with EZH2 inhibitor GSK-126 for H3K27me3 (upper) and total Histone H3 (n=3 biological replicates) or H3K27ac (bottom) and total Histone H3 (n=3 biological replicates) (Right) Quantification of Western Blot by one-way ANOVA, *p<0.05, ****p<0.0001. (**B**) MA plot describing differential methylation due to GSK126 treatment in cultured

Figure 7 continued on next page

Figure 7 continued

CGNs (FDR <0.05 and $|Log_2FC|>1$) (n=3 biological replicates). (**C**) Metagene plots for H3K27me3 peaks of DMSO and 5 μM GSK-126 treated CGNs at genes within clusters (Left) All promoters with H3K27me3, (Center) H3K27me3 Up from DIV1-7, and (Right) H3K27me3 Down from DIV1-7, described in ***Figure 5E***. (**D**) Relationship between gene expression changes during CGN maturation from DIV0-7 (y-axis) and due to GSK-126 treatment from DIV1-5 (x-axis). Pink lines represent the linear regression and dotted lines show the confidence interval. (**E**) Representative CUT&RUN tracks (Upper) and (Lower) RNA-seq tracks for example gene with Unchanged H3K27me3 from DIV1-7 – Jag1, gene within cluster 'H3K27me3 Up from DIV1-7' – Ebf3 and 'H3K27me3 Down from DIV1-7' - Gabrd, for DMSO and GSK126 treated CGNs. (**F**) CUT&RUN tracks at putative Mycn enhancer cluster and putative Grin2c enhancer. (**G**) Violin plot showing the distribution of Log_2FC of gene expression between DMSO and GSK-126 treated CGNs from either DIV1-5 (left) or DIV3-5 (right) as a function of clustering performed in ***Figure 5D*** (one-way ANOVA, **p<0.005, ***p<0.0005, ****p<0.0001).

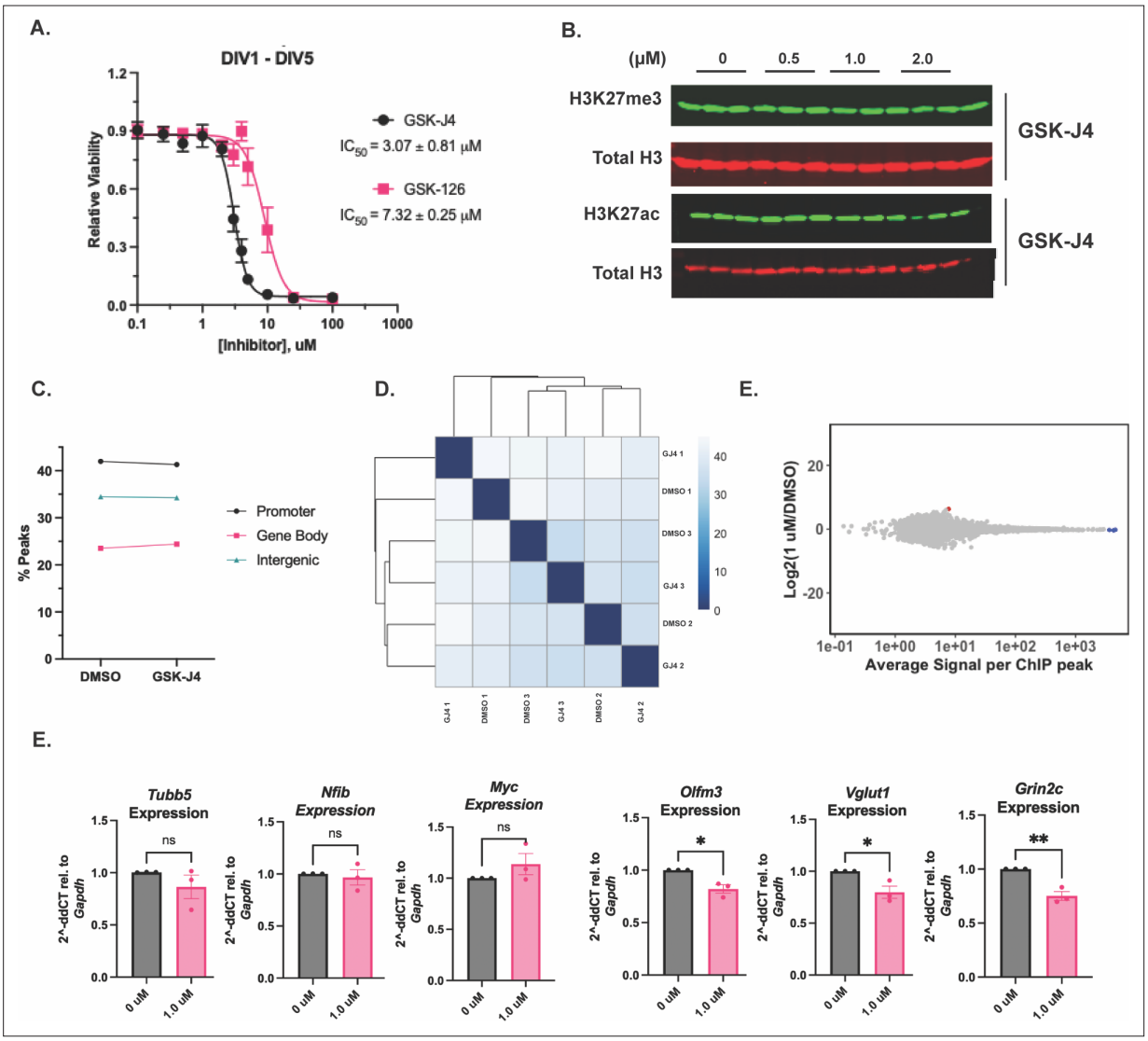

Figure 7—figure supplement 1. GSK-J4 treatment at 1 μM does not affect genome wide levels of histone H3 lysine 27 trimethylation (H3K27me3), but influences the expression of late cerebellar granule neuron (CGN) genes. (**A**) Cell Titer Glo Assay for CGNs treated with GSK-126 or GSK-J4 at DIV1 and measured at DIV5 (n=2 biological replicates). (**B**) Western blot of acid-extracted histones from CGNs treated for H3K27ac and total Histone H3 (n=3 biological replicates). (**C**) Percentage of H3K27me3 peaks annotated by genomic location – promoter, gene body, or distal intergenic region. (**D**) Sample-to-sample distance plot for H3K27me3 CUT&RUN peaks for DMSO and GSK-J4 treated samples and their biological replicates. (**E**) MA plot showing differential peak enrichment between DMSO and GSK-J4 treated CGNs. (**F**) RT-qPCR for early genes *Tubb5*, *Nfib*, and *Myc* (left) and late genes *Olfm3*, *Vglut2*, and *Grin2c* (right) for CGNs treated with DMSO or GSK-J4 (n=3 biological replicates). Unpaired *t*-test, *<0.05, *p<0.005.

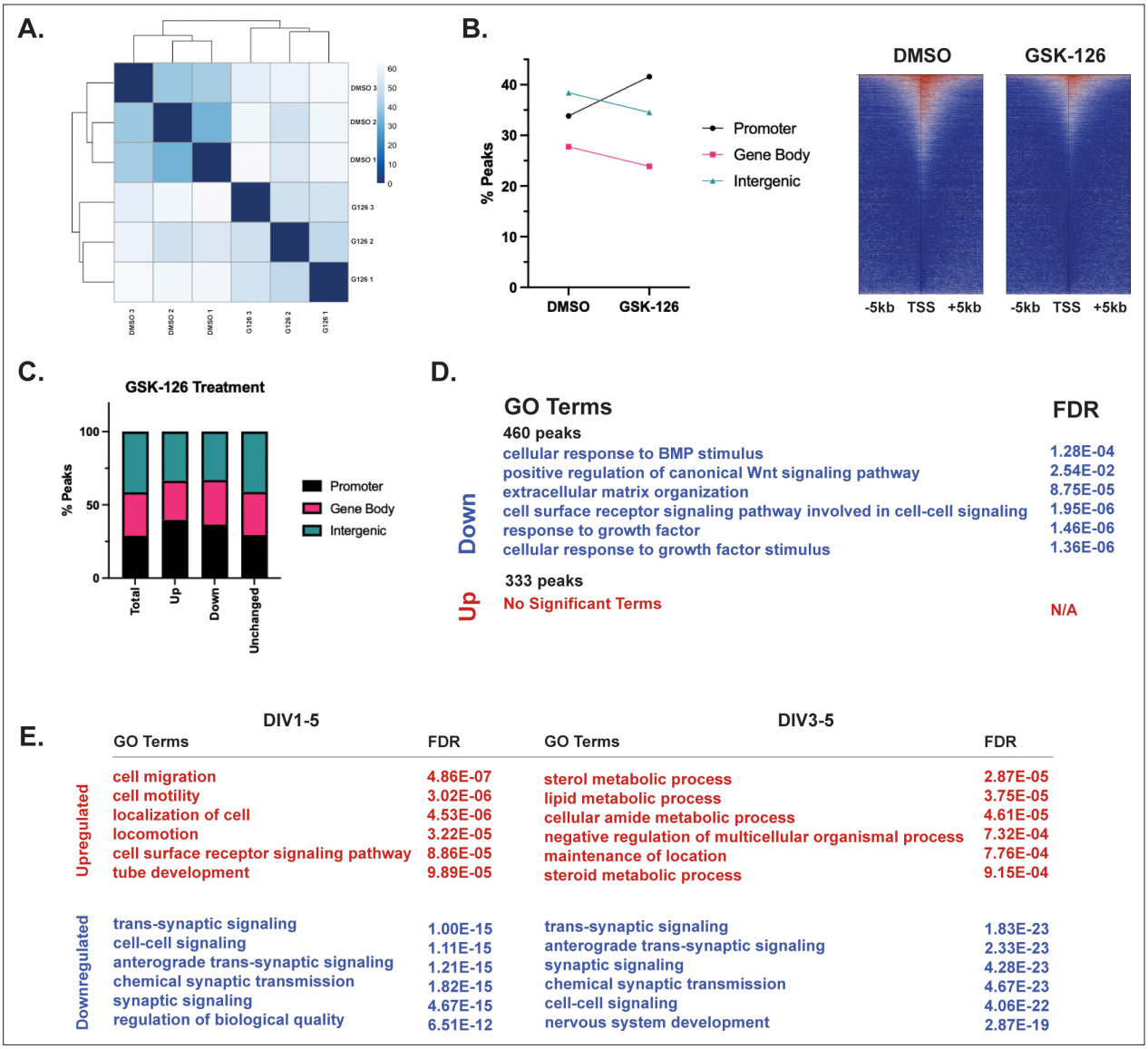

Figure 7—figure supplement 2. EZH2 inhibition redistributes histone H3 lysine 27 trimethylation (H3K27me3) across cerebellar granule neuron (CGN) genome. (**A**) Sample-tosample distance for H3K27me3 CUT&RUN peaks for DMSO and GSK-126 treated CGNs in culture (n=3 biological replicates). (**B**) (left) H3K27me3 peaks annotated by genomic location – promoter, gene body, and distal intergenic regions. (right) Heatmap showing H3K27me3 peak coverage for CGNs treated with DMSO or GSK-126 within a window of TSS +/− 5 kb (left), Percentage of H3K27me3 peaks annotated by genomic location – promoter, gene body or distal intergenic region (right). (**C**) Percentage of differential H3K27me3 peaks between DMSO and GSK-126 treated CGNs, annotated by genomic region. (**D**) Gene Ontology (GO) Terms and FDR associated with genes nearest to peaks described as 'Up' or 'Down' in ***Figure 6***. (**E**) GO Terms and FDR associated with genes upregulated or downregulated due to GSK-126 treatment at DIV1-DIV5 (left) and DIV3-DIV5 (right).